

Article

Barley Plants Overexpressing *Ferrochelatases* (*HvFC1* and *HvFC2*) Show Improved Photosynthetic Rates and Have Reduced Photo-Oxidative Damage under Drought Stress than Non-Transgenic Controls

Dilrukshi S. K. Nagahatenna ¹, Boris Parent ², Everard J. Edwards ³ , Peter Langridge ^{1,4,*} 
and Ryan Whitford ¹ 

¹ School of Agriculture, Food and Wine, University of Adelaide, Waite Campus, PMB1, Glen Osmond SA 5064, Australia; dilu.nagahatenna@adelaide.edu.au (D.S.K.N.); ryan.whitford@adelaide.edu.au (R.W.)

² Unité Mixte de Recherche 759 Laboratoire d'Ecophysiologie des Plantes sous Stress Environnementaux, INRAE, F-34060 Montpellier, France; boris.parent@inrae.fr

³ CSIRO Agriculture & Food, Locked Bag 2, Glen Osmond SA 5064, Australia; everard.edwards@csiro.au

⁴ Wheat Initiative, Julius-Kühn-Institute, Königin-Luise-Str 19, 14195 Berlin, Germany

* Correspondence: peter.langridge@adelaide.edu.au; Tel.: +61-88313-7171; Fax: +61-88313-7102

Received: 14 August 2020; Accepted: 3 September 2020; Published: 8 September 2020



Abstract: We investigated the roles of two *Ferrochelatases* (FCs), which encode the terminal enzyme for heme biosynthesis, in drought and oxidative stress tolerance in model cereal plant barley (*Hordeum vulgare*). Three independent transgenic lines ectopically overexpressing either barley *FC1* or *FC2* were selected and evaluated under well-watered, drought, and oxidative stress conditions. Both *HvFC1* and *HvFC2* overexpressing transgenics showed delayed wilting and maintained higher photosynthetic performance relative to controls, after exposure to soil dehydration. In each case, *HvFC* overexpression significantly upregulated the nuclear genes associated with detoxification of reactive oxygen species (ROS) upon drought stress. Overexpression of *HvFCs*, also suppressed photo-oxidative damage induced by the deregulated tetrapyrrole biosynthesis mutant *tigrina*^{d12}. Previous studies suggest that only *FC1* is implicated in stress defense responses, however, our study demonstrated that both *FC1* and *FC2* affect drought stress tolerance. As FC-derived free heme was proposed as a chloroplast-to-nuclear signal, heme could act as an important signal, stimulating drought responsive nuclear gene expression. This study also highlighted tetrapyrrole biosynthetic enzymes as potential targets for engineering improved crop performance, both in well-watered and water-limited environments.

Keywords: tetrapyrrole; ferrochelatase; heme; barley; ROS; photosynthesis; drought; retrograde signal

1. Introduction

Drought is one of the major abiotic stress factors that adversely affects plant growth and limits crop yield [1]. Therefore, improving drought tolerance of major crops such as cereals is a primary objective for plant breeding. Improved crop performance under water-limited conditions is necessary to satisfy food demands that are a consequence of a growing world population. The incidence and severity of drought events in many rain-fed cereal growing areas is likely to increase in the face of a changing climate. Photosynthesis is a primary cellular process that is directly affected by cellular water status [2]. Drought stress and the consequent reduction in cellular water status significantly reduces photosynthetic rate, by limiting CO₂ diffusion through the stomata, and potentially induces

secondary effects like oxidative stress, which can damage the photosynthetic machinery [3]. Ultimately, this leads to substantial yield losses. Drought-tolerant C_3 plants evolved efficient strategies to avoid or respond to drought stress, for example, acclimation mechanisms allow plants to minimize water loss from transpiration. This can occur as a result of stomatal closure, adjusted leaf architecture, reduced leaf growth, and by shedding older leaves [3]. Plants can also avoid dehydration by maximizing water uptake as a result of favored root, relative to shoot growth [4]. Plants exhibiting developmental plasticity can also escape drought by completing their life cycle before the drought stress becomes lethal. Increased levels of osmoprotectants such as proline, glycine, betaine, and polyols, allow plants to maintain turgor and protect cells from plasmolysis [3]. Similarly, high levels of antioxidants can mitigate ROS damage [5]. Drought tolerance is a complex phenotype under complex genetic control [6,7], as evidenced by the multitude of gene expression changes upon exposure to stress. Such transcriptional changes are necessary for ‘reprogramming’ whole plant performance upon stress. Understanding the physiological basis for drought tolerance as well as the underlying genes and biochemical mechanisms is a prerequisite towards developing superior crop varieties.

The tetrapyrrole biosynthesis pathway supplies essential compounds, chlorophyll, and heme, for photosynthesis [8] (Figure 1). Chlorophyll is the most abundant pigment in plants and is necessary for photochemical energy conversion, which drives photosynthesis. Heme, on the other hand, is an integral component of photosynthetic and respiratory cytochromes that is involved in electron transport [9,10]. Unlike chlorophyll, heme is important for many cellular functions, including acting as a co-factor for enzymes that are able to detoxify ROS [11]. Recently, it was proposed that a sub-pool of heme might serve as a retrograde signal, triggering photosynthesis-associated nuclear gene expression [12–14]. Both chlorophyll and heme are produced in the chloroplast. For their synthesis, 5-aminolevulinic acid (ALA), the initial common tetrapyrrole precursor is converted, through a series of reactions, into protoporphyrin IX (Proto IX). Insertion of Mg^{2+} into Proto IX, through the action of Mg-chelatase, leads to the production of chlorophyll, whereas the insertion of Fe^{2+} by Ferrochelatase (FC), results in the production of heme [15] (Figure 1).

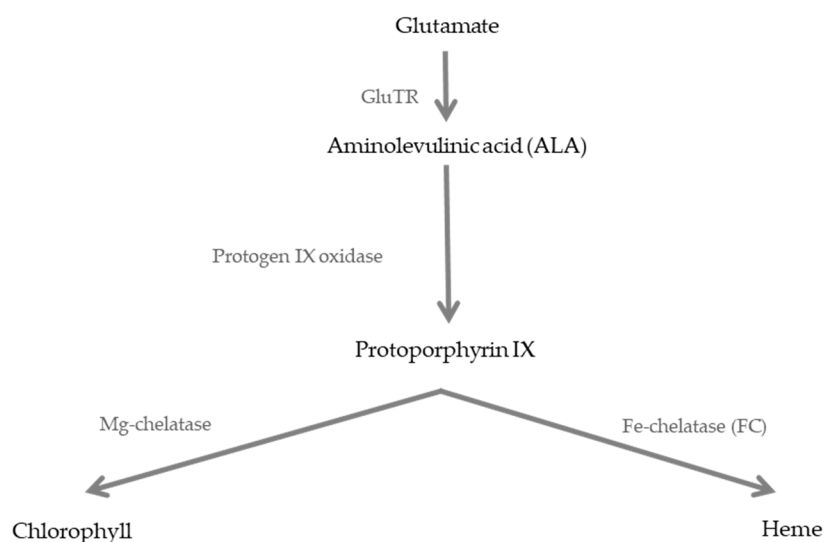


Figure 1. The tetrapyrrole biosynthesis pathway with the major end-products (bold text) and some catalytic enzymes. GluTR—glutamyl-tRNA reductase and Protoporphyrin IX oxidase—Protoporphyrinogen IX oxidase.

In all plant species investigated so far, FC, the terminal enzyme for heme biosynthesis, is encoded by two genes [16,17]. Both FC isoforms have similar catalytic properties, substrate affinity, and specificity [18], but seem to have different expression profiles and subcellular localization. For instance, *FC1* is ubiquitously expressed in all plant tissues, including roots, whereas *FC2* is only found in aerial

portions of the plant [16,19–22]. Transcriptional reporter gene fusions showed that *Arabidopsis FC1* is induced in response to wounding, oxidative stress, and viral infection. In contrast, *FC2* is repressed or remains unchanged under these stress conditions [16,21]. Furthermore, *FC2* is strictly confined to the chloroplast, but *FC1* is transported to both chloroplast and mitochondria [19,23–26]. These findings led the authors to propose that two physiologically distinct heme pools are synthesized by each of these FCs, with only *FC1*-derived heme being implicated in stress response. However, there is still disagreement regarding these proposed distinct roles for FC isoforms, as outlined in subsequent studies. For example, Lister et al. (2001) [27] were unable to detect *FC1* in *Arabidopsis* mitochondria, whilst in cucumber, both *FC1* and *FC2* were found to be solely targeted to chloroplasts [28]. Therefore, it is now timely that their respective roles are being investigated more broadly. Gaining this knowledge in monocots is crucial for determining whether these genes are ideal targets for engineering stress tolerance in economically important cereals.

Several genetic and biochemical studies proposed that increased flux through the heme branch of the pathway improves tolerance to drought stress [29–34]. To understand the roles for these genes in drought and oxidative stress responses, we used barley, a major global crop but also a model for wheat. Two FCs were identified and cloned from barley cultivar Golden Promise (GP) [35]. Transgenic lines ectopically overexpressing either *HvFC1* or *HvFC2* were generated with three independent lines selected for each FC isoform [35]. Intriguingly, we found that overexpression of either *HvFC1* or *HvFC2* improves photosynthetic performance under non-stressed conditions, implying that both FCs play crucial roles in photosynthesis [35]. Transgenic lines were then evaluated under drought and oxidative stress. Oxidative stress was induced either by herbicide (Paraquat) application or genetically via the exposure of a deregulated tetrapyrrole biosynthetic mutant, *tigrina^{dt12}*, to a dark to light shift. Here, we report that ectopic overexpression of either *HvFC1* or *HvFC2*, improves photosynthetic capacity, both under well-watered and drought conditions, with this being a likely consequence of increased tolerance to photo-oxidative damage.

2. Materials and Methods

2.1. Genetic Materials

Barley transgenic lines (cv. Golden Promise (GP)) ectopically overexpressing either *HvFC1* or *HvFC2* were generated by *Agrobacterium*-mediated delivery of pMDC32-*HvFC1* and pMDC32-*HvFC2* constructs (Figure S1), as described by Tingay et al. (1997) and Matthews et al. (2001) [36,37]. Twenty-nine T₀ transformants were successfully generated and their transgene integrity was confirmed by PCR, using primers specific for hygromycin resistance gene (*Hyg*) and transgenes (Table S1). Transgene copy number and total *HvFC1* and *HvFC2* expression levels were analyzed by Southern hybridization and quantitative RT-PCR, respectively [35]. T₁ and T₂ plants originating from each independent transformation event was screened for transgene copy number and expression. Eventually, three single-copy, stable overexpression lines were selected for each FC isoform from T₂ generation [35] and evaluated for stress tolerance. For detailed information on the experimental procedure please refer to Nagahatenna et al. (2020) [35].

2.2. Plant Growth and Stress Conditions

For *HvFC* gene expression analysis under oxidative stress, barley (*Hordeum vulgare* L.cv. Golden promise) plants were grown in pots containing coco-peat and field soil (50:50, v/v), supplemented with slow-release fertilizer pellets (Mini Osmocote; Smoult Horticultural Suppliers, Adelaide, Australia), at 2 g per liter soil volume. All replicates were randomly allocated in the controlled environment growth chamber to minimize positional effect, and growth conditions were maintained at 20–18 °C day/night temperature, 50–60% relative humidity, 460 μmolm⁻²s⁻¹, and a 12:12 h photoperiod. In all drought assays, control plants were grown under the conditions as outlined above.

For evaluating performance of barley transgenics that ectopically overexpressed *HvFCs* upon drought stress, one untransformed control, null segregant, and transgenic seed was planted together in a single pot (25.5 cm in diameter and 23.5 cm in height), therefore, exposing all plants to the same soil conditions. A total of five pot replicates were analyzed per time point and per treatment. Each pot was lined with a polythene sheet to ensure no water added to the pot was lost due to drainage, so that all plants within the pot had access to the same soil water moisture. All plants were grown under conditions as outlined above.

For gene expression analysis involving *tigrina*^{d12}, plants were grown under 24 h continuous light. To investigate the role of *HvFC* overexpression on tetrapyrrole-mediated oxidative stress, control barley (*Hordeum vulgare* L. cv. Golden promise and cv. Bonus), transgenic lines (T₂), non-transgenic and transgenic *tigrina*^{d12} overexpressing either *HvFC1* or *HvFC2*, were also grown under 24 h continuous light, with all other conditions controlled as outlined above.

2.3. Drought Assay

Each pot was watered equally to maintain similar pot weight for six weeks and then water was withheld. In order to identify variation of soil water potential in each pot upon drought stress, a calibration experiment was conducted concurrently. In this calibration experiment, control (cv. Golden Promise) plants were planted in similar polythene lined pots containing the same amount of soil and were grown under the same growth conditions, as outlined above. Predawn leaf water potential was measured daily, using a plant water status console (Model 3000, Soil moisture Equipment Corp., P.O. Box 30025, Santa Barbara, CA 93105, USA), until the plants wilted. This predawn leaf water potential was considered to be equivalent to the soil water potential in each pot [38]. Furthermore, pot weight was measured daily to determine the soil moisture corresponding to the respective soil water potential. Based on the soil humidity and soil water potential, a water release curve of this soil mixture was constructed (Figure S2). In the drought assay, pot weights were monitored daily upon drought stress to identify corresponding soil water potential, as indicated by the water release curve. A soil water potential of -0.6 MPa was maintained for 1 week and then plants were rewatered (Figure 2). Measurements were taken before stress, 2, 5, 8, and 15 days post water-withholding as well as after rewatering (18 days post water-withholding; Figure 2). These time-points represent fully irrigated (0), -0.1 , -0.3 , -0.6 , and -0.6 MPa, and fully rewatered soil water potentials.

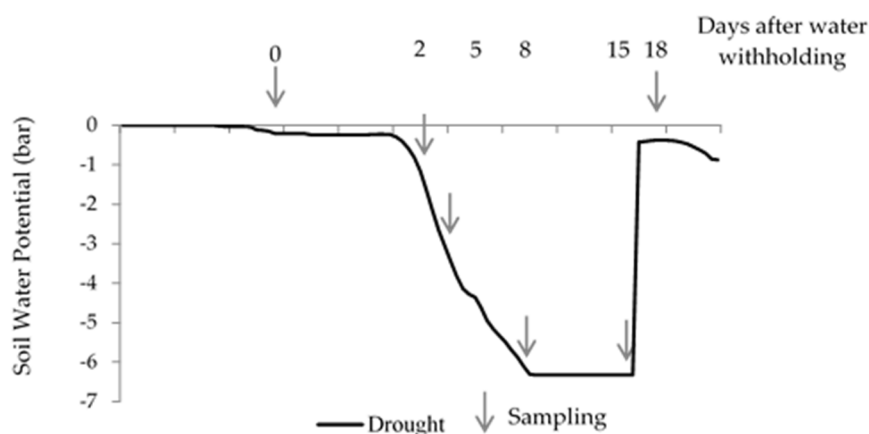


Figure 2. Variation of the soil water potential before, during, and after drought stress. Four weeks after planting, watering was withheld. Minus 6 MPa soil water potential was maintained for a week, and then plants were rewatered to initial soil water potential. Arrows indicate different time-points where measurements were taken.

2.4. Paraquat Treatment

The second leaf from the top of the primary tiller of the 3-week-old control and transgenic lines were dipped in a 20 μM Paraquat solution (Sigma, NSW, Australia) for 1 min under dark, and re-exposed to 24 h continuous light of constant intensity. The degree of necrosis in transgenics, relative to the controls was evaluated following herbicide treatment. Transcriptional responses of *HvFC1* and *HvFC2* to Paraquat-induced oxidative stress was analyzed in the leaves of the control plants through quantitative RT-PCR.

2.5. Screening and Evaluating *Tigrina*^{d12} Mutants Overexpressing *HvFC1* and *HvFC2* Under Tetrapyrrole-Mediated Oxidative Stress

To investigate the role of the *HvFC* under tetrapyrrole-mediated oxidative stress, a representative transgenic line for *HvFC1* and *HvFC2* was crossed with *tigrina*^{d12}. Seeds from non-transgenic and transgenic *tigrina*^{d12} mutants (F_2), *HvFC* overexpressing lines (T_2) and control barley (*Hordeum vulgare* L.cv. Golden promise and cv. Bonus) were grown on a wet petri plate for 5 days, under continuous darkness. Cotyledons were removed under a safe green light and were illuminated under UV light to identify homozygous mutants in F_2 segregating population. Photographs were taken with a Canon 60D digital camera. Images were analyzed for red fluorescence intensity, using the ImageJ software (1.33 version; <http://imagej.nih.gov/ij/>).

Homozygous F_2 *tigrina*^{d12} mutant phenotypes were confirmed using a cleaved amplified polymorphic sequence (CAPS) marker, designed to the causative mutation in the *FLU* gene [39]. PCR analysis was conducted with *FLU* and transgene specific primers. For the analysis using the CAPS markers, the PCR product was digested with *Hae* III restriction endonuclease (NEB, Victoria, Australia) at 37 °C for 2 h, and 65 °C for 10 min. PCR products before and after digestion were analyzed in 2% agarose gel and visualized by staining with ethidium bromide.

Mutant seedlings, which contain *HvFC* transgenes, were identified by using a dominant transgene-specific PCR marker. The primer sequences used are described in Supplementary Materials (Table S1). In order to investigate the effect of *HvFC* overexpression on tetrapyrrole-mediated oxidative stress, 3-week-old transgenic *tigrina*^{d12} mutants with all of the above-mentioned controls were grown under 24 h continuous light with 450 $\mu\text{mol m}^{-2}\text{s}^{-1}$ photosynthetically active radiation. Then, the plants were subjected to 24 h dark period and re-illuminated, before measuring chlorophyll fluorescence, and sampling for chlorophyll content.

2.6. Chlorophyll Content

Chlorophyll was extracted from leaf tissues using dimethyl sulfoxide (DMSO; Sigma, NSW, Australia) and determined spectrophotometrically, according to Hiscox and Israelstam (1979) [40]. The total chlorophyll content was calculated using the following equation. Total chlorophyll (g L^{-1}) = $0.0202 A_{645} + 0.00802 A_{663}$ (A_{645} and A_{663} are absorbance at 645 and 663 nm).

2.7. Chlorophyll Fluorescence

Chlorophyll fluorescence parameters were measured using a pulse-amplitude-modulated photosynthesis yield analyzer (Mini-PAM, Walz, Effeltrich, Germany), with a dark leaf clip, to ensure all measurements were taken at the same distance from the leaf. Maximum quantum yield of PSII photochemistry (calculated as ratio $F_v/F_m = (F_m - F_o)/F_m$) was determined by applying an 800 ms saturating light pulse to leaves, under predawn conditions.

2.8. Measurements of Relative Water Content (RWC)

For leaf RWC measurement, leaves were excised between 09.00 h and 10.00 h, and their fresh weight was measured immediately. Rehydrated weight was determined by floating them in deionized

water at 4 °C overnight. Leaf dry weight was measured by oven-drying at 80 °C for 48 h. The RWC was calculated as follows: $RWC (\%) = (\text{fresh weight} - \text{dry weight}) / (\text{rehydrated weight} - \text{dry weight}) \times 100$.

2.9. Photosynthetic Measurements

In vivo gas exchange parameters were measured in developmentally equivalent, fully expanded leaves, in 4- to 6-weeks old plants using a LI-6400 portable photosynthesis system (Licor inc, Lincoln, NE, USA). The conditions of the leaf cuvette were set to a light intensity of 2000 $\mu\text{mol m}^{-2} \text{s}^{-1}$, humidity of 50–60%, temperature 25 °C, and reference air CO₂ concentration of 400 $\mu\text{mol s}^{-1}$. The measurement period was from 09.00 h to 17.00 h. Leaf area in the cuvette was measured and gas exchange parameters per unit leaf area were recalculated. Instantaneous WUE and carboxylation efficiency (CE) were calculated based on the gas exchange parameters. Instantaneous WUE = photosynthesis rate under saturated light/transpiration rate, $CE = A_{\text{sat}}/\text{intracellular CO}_2 \text{ concentration}$.

2.10. Gene Expression Analysis

Total RNA was extracted from leaf tissues of 3-weeks old control and transgenic plants before and during drought stress, as well as post oxidative stress, using an RNeasy plant extraction kit (Qiagen, VIC, Australia). cDNAs were prepared using SuperScript III reverse transcriptase (Invitrogen, Carlsbad, CA, USA). Gene expression was analyzed by quantitative RT-PCR, using primers from the coding regions of *HvFC1*, *HvFC2*, *Catalase (Cat)*, and *Superoxide dismutase (Sod)*, as described by Burton et al., (2004) [41]. mRNA copy number for each tested gene was normalized against four control genes (*GAPDH*, *HSP70*, *cyclophilin*, and *tubulin*), as described by Burton et al., (2004) [41]. Primer sequences used in these experiments are described in the Supplementary Materials (Table S1). Relative expression was calculated using the $2^{-\Delta\Delta CT}$ method, as described by Schmittgen and Livak (2008) [42], and fold change in target gene expression was normalized to endogenous reference genes and to the untreated wild-type control.

2.11. Statistical Analysis

All data were statistically analyzed by either one-way or two-way ANOVA, using GenStat 12.1 software (England, UK), and mean differences were compared through LSD test. Differences were considered to be statistically significant when $p < 0.05$.

3. Results

3.1. Overexpression of *HvFC1* and *HvFC2* Maintained Higher Leaf Water Status and Water Use Efficiency Under Drought Stress, Independent of Stomatal Closure

As an initial step towards understanding the role of FCs in drought stress responses, two FCs were identified in barley [35]. Our bioinformatics analysis revealed that two FCs are localized on separate chromosomes; *HvFC1* on 5H and *HvFC2* on 1H. Barley transgenic lines (cv. GP) ectopically overexpressing *HvFC1* and *HvFC2* were generated by cloning the coding regions of FC into the pMDC32 vector, under the control of the $2 \times 35S\text{CaMV}$ promoter [35]. Twenty-nine independent T₀ transgenic lines were screened for transgene copy number and expression. Three single copy, independent transgenic events, each ectopically overexpressing either *HvFC1* or *HvFC2*, were selected [35] and evaluated upon drought stress. The gradual reduction in soil water potential over the period of the drought stress (Figure 2) was inferred by using a standardized drying curve (Figure S2).

This drying curve was previously determined to represent the relationship between predawn leaf water potential, pot weight, and the particular soil characteristics used in this experiment. We first made qualitative observations on the relative time to wilting. Visual inspection revealed controls reversibly wilted at -0.6 MPa soil water potential (8 days post water-withholding), whereas neither *HvFC1* nor *HvFC2* overexpressing transgenics exhibited wilting symptoms. This can be seen in Figure 3 in the day 8 image (b,e), where the representative transgenic line for either *HvFC1* or *HvFC2* at the

rear of the pot remain erect, while those at the front were wilted (untransformed controls (WT) and null segregants).

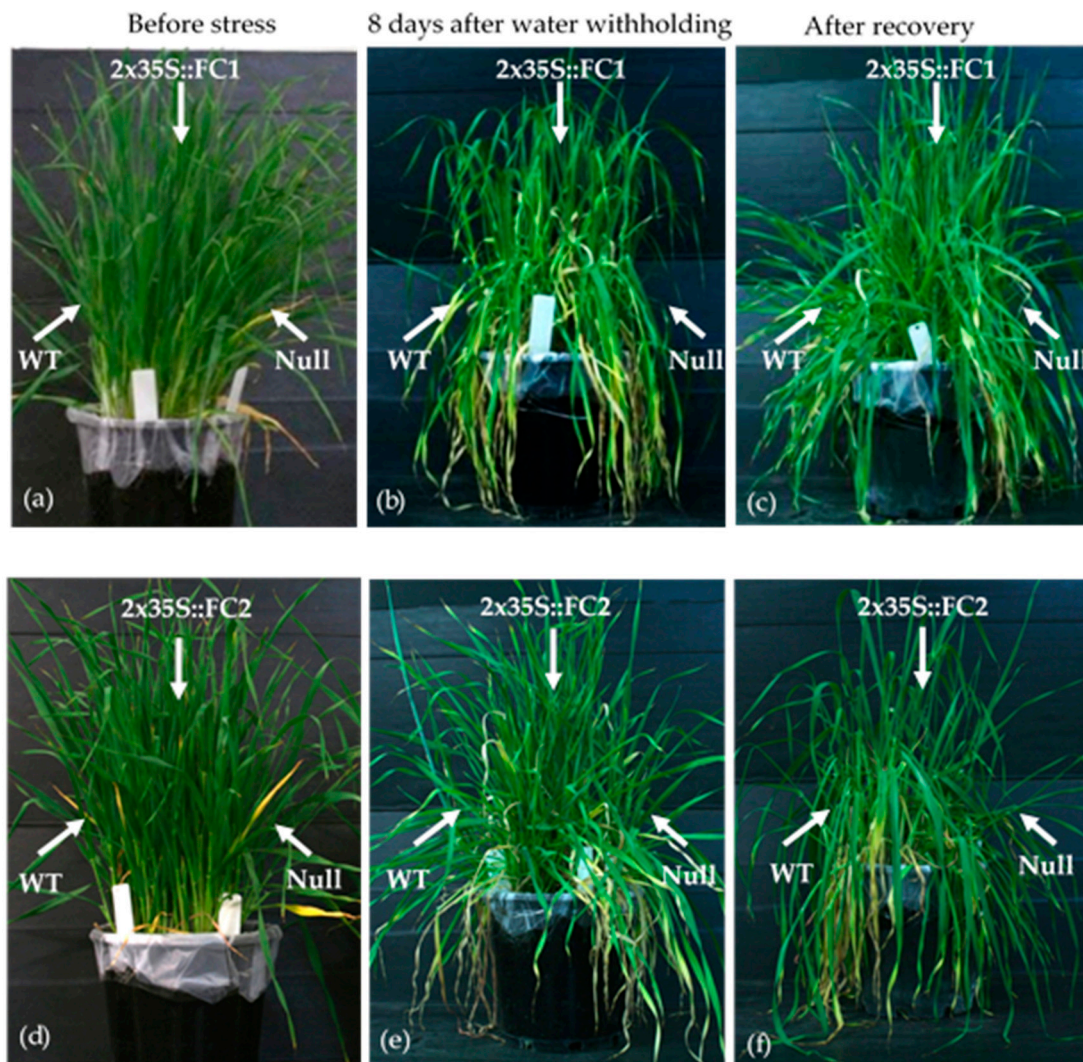


Figure 3. Phenotypes of the representative control plants and transgenic lines (T_2) grown under controlled environmental conditions in the absence of stress (a,d), 8 days post water-withholding (b,e), and after re-watering (c,f). The control plants were reversibly wilted, 8 days after withholding water, whereas both types of transgenics did not wilt.

Given that a plant's wilting point is in part governed by leaf water content, we measured leaf relative water content (RWC) before, during, and after water deficit stress. No significant difference in leaf RWC was observed between the transgenics and controls before drought stress and after rewatering. However, results revealed that both *HvFC1* and *HvFC2* transgenics (calculated as an average of data from three transgenic events per construct) had a higher leaf RWC during drought stress, than the controls (Figure 4a). At -0.6 MPa soil water potential (day 8), transgenics on average had 10–12% higher leaf RWC, compared to controls.

Water is continually lost to the atmosphere via transpiration and one of the mechanisms that protects plants from excessive water loss is the stomatal closure. Therefore, we investigated whether *HvFC* transgenics had a higher leaf RWC, as a consequence of lower stomatal conductance (g_s), relative to controls. However, *HvFC1* transgenics showed greater g_s , before and during the early phases of drought stress (2 and 5 days post water-withholding) relative to controls (Figure 4b). This

observed difference ceased at a soil water potential of -0.6 MPa (8 days), and increased once more, post rewatering. A similar trend, albeit not statistically significant, was observed between *HvFC2* transgenics and controls. These findings indicated that the higher leaf RWC was unlikely to be a consequence of reduced g_s for *HvFC1* and *HvFC2* overexpressing transgenics. Collectively, these findings indicate that both *HvFC* transgenics improved leaf water status during drought stress, when compared to controls. The observed differences in g_s between *HvFC1* and *HvFC2* transgenics might be a consequence of the alternate modes of action for FC isoforms.

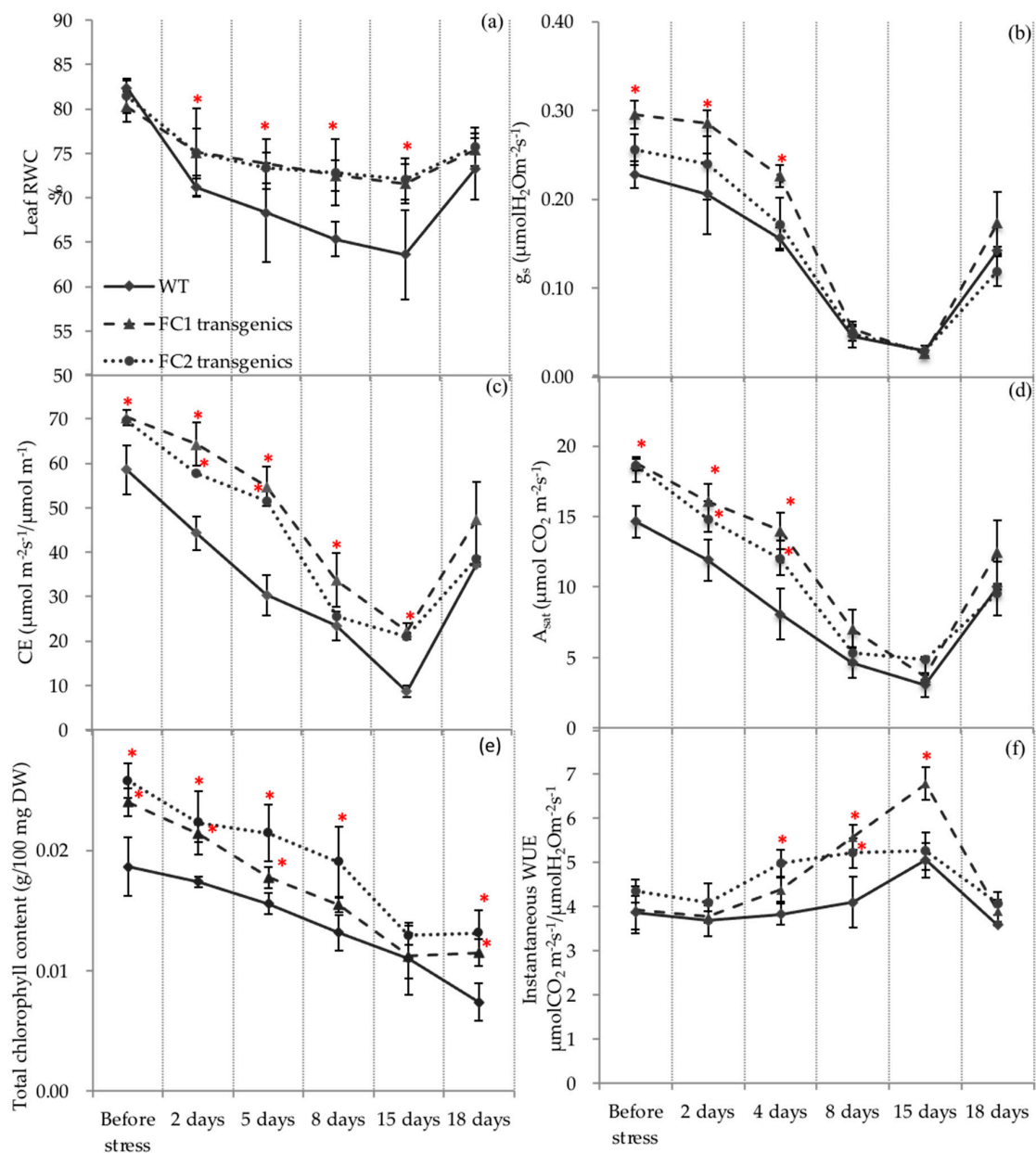


Figure 4. *HvFC* overexpressing transgenics maintained higher leaf water status and photosynthetic performance relative to controls upon drought. Physiological traits measured include—(a) leaf relative water content (RWC), (b) stomatal conductance, (c) instantaneous carboxylation efficiency, (d) carbon assimilation rate, (e) total chlorophyll content, and (f) instantaneous water use efficiency (WUE) relative to wild-type (WT) control plants upon drought stress. The data are shown as mean \pm standard error (SE) of five plants for each of the three independent transgenic lines, per construct and WT. Asterisks indicate a statistically significant difference between the transgenics and controls, at $* p < 0.05$ based on two-way ANOVA.

3.2. *HvFC1* and *HvFC2* Overexpressing Transgenics Maintained Higher Photosynthetic Activity in the Well-Watered Conditions and Upon Dehydration

Water and CO₂ are essential substrates for photosynthesis. Therefore, we investigated whether the observed positive water status and enhanced g_s in *HvFC* transgenics has the capacity to improve photosynthesis. Measurements of CE revealed that both *HvFC1* and *HvFC2* transgenics had a significantly higher photosynthetic capacity, relative to wild-type controls, before and during the early phases (2–5 days post water-withholding) of drought stress, and even after 1 week, at -0.6 MPa soil water potential (15 days post water-withholding) (Figure 4c). This finding extended to the photosynthesis rate under saturated light, whereby both *HvFC1* and *HvFC2* transgenics showed a significantly higher A_{sat} , before and 2 to 5 days post water-withholding, relative to the controls (Figure 4d). The improvement in A_{sat} was between 3 and 4 $\mu\text{mol m}^{-2}\text{s}^{-1}$ in both transgenics, relative to wild-type (Figure 4d).

The amount of photosynthetic pigment was also important for photosynthesis, considering they were responsible for light energy absorption. Both *HvFC1* and *HvFC2* overexpressing transgenics exhibited a significantly higher chlorophyll content before stress, at -0.1 and at -0.3 MPa soil water potential (2 to 5 days after post water-withholding), as well as after rewatering, relative to the controls (Figure 4e). Importantly, in *HvFC1* transgenics (calculated as an average of data from three transgenic events per construct), the instantaneous WUE was unchanged, before and up to 5 days post water-withholding, as well as after rewatering (Figure 4f). Only marginal increases in WUE were observed from 8 to 15 days post water-withholding. In contrast, *HvFC2* transgenics exhibited significantly higher WUE, 5 to 8 days post water-withholding. These findings suggest that *HvFC1* and *HvFC2* differentially affect WUE. However, collectively these results suggest that the overexpression of both *HvFC*'s have the capacity to maintain higher photosynthetic activity relative to controls, under both well-watered and drought stress conditions.

3.3. Overexpression of *HvFCs* Invokes Expression of ROS Detoxification Markers

Impairment of photosynthetic electron transport and increased photorespiration lead to photo-oxidative damage, upon dehydration [3]. The ability to minimize cellular oxidative damage is an important protective strategy. To investigate whether both types of transgenics have the ability to prevent drought-mediated oxidative stress, transcriptional responses of genes associated with ROS detoxification were analyzed in controls versus a representative transgenic line for *HvFC1* and *HvFC2*, before, during, and after water-deficit stress. Transcripts targeted for analysis included *Cat* and *Sod*, as they were previously shown to be transcriptionally responsive to drought and encode proteins that are important for ROS detoxification [43]. *Cat* expression in *HvFC1* transgenics was significantly repressed ($p < 0.05$) as compared to the control plants, both before stress and up to 8 days post exposure to drought (Figure 5a). As stress progressed up to 15 days, this trend reversed, whereby *Cat* was significantly upregulated ($p < 0.05$) in the transgenic, relative to the control. However, this observation was not statistically significant when comparing plants overexpressing *HvFC2* to control plants, both before stress and up to 8 days post exposure to drought (Figure 5c). Analysis of *Sod* mRNA levels in *HvFC1* transgenics revealed that *Sod* is transcriptionally upregulated, both at 8 and 15 days post water-withholding, with no significant difference observed in transcriptional activity before the onset of stress (Figure 5b). This contrasted with *Sod* transcription in *HvFC2* transgenics, which showed a significant downregulation ($p < 0.05$), when compared to control plants before stress (Figure 5c). Similar to *HvFC1* transgenics, *Sod* was transcriptionally upregulated in *HvFC2* transgenics, after 8 days of exposure to drought stress. These findings showed that both FC isoforms had the capacity to modulate nuclear encoded transcription of ROS detoxification enzymes, upon drought stress.

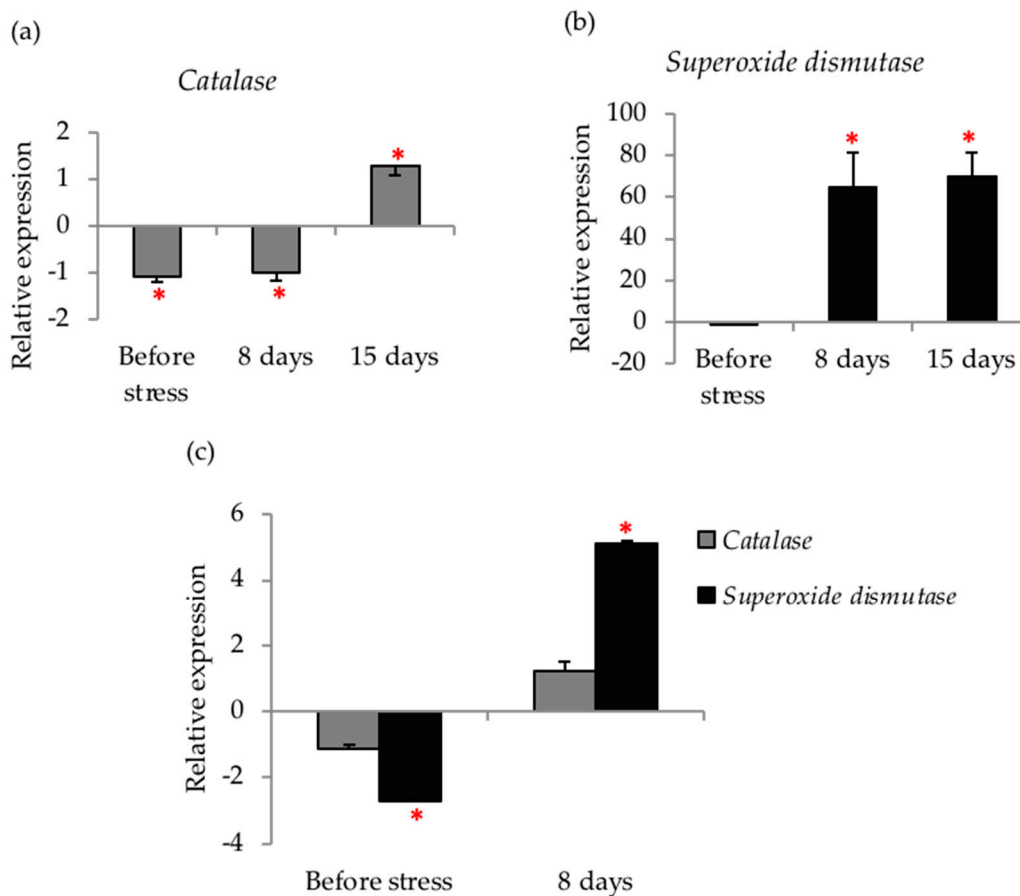


Figure 5. Transcriptional responses of ROS detoxification enzymes, catalase, and superoxide dismutase, in a representative transgenic line, each ectopically overexpressing *HvFC1* (a,b) or *HvFC2* (c) under drought stress, relative to WT control. The data are shown as mean \pm standard error (SE) of 3 different plants. Asterisks indicate statistically significant expression difference between transgenics and WT control, at $* p < 0.05$, based on two-way ANOVA.

3.4. *HvFC* Overexpression Protects Plants from Tetrapyrrole-Induced Photo-Oxidation

The apparent ability of both *HvFC* transgenics to improve ROS detoxification upon drought stress, prompted us to investigate whether ectopic overexpression of *HvFCs* improved oxidative stress tolerance. This was tested by exposing *HvFC* transgenic leaves to 20 μ M paraquat and visually assessing leaf photo-bleaching, relative to wild-type and null controls. Qualitative observations of leaf photo-bleaching as a time-course, post-paraquat treatment, revealed no significant differences in leaf photo-bleaching between both *HvFC1* and *HvFC2* transgenics, relative to their respective controls (data not shown). This would indicate that these transgenics did not improve tolerance to paraquat-induced oxidative stress, although visual differences between transgenics and controls might be observed if lower concentrations of paraquat were used.

Under stress, plants also undergo oxidative stress, generated by photo-sensitizing tetrapyrrole intermediate accumulation [44,45]. In order to investigate whether ectopic overexpression of *HvFCs* contribute to tetrapyrrole-induced oxidative stress tolerance, we used the *tigrina*^{d12} mutant. In *tigrina*^{d12}, tetrapyrrole biosynthesis is deregulated and consequently these plants accumulate the highly photo-sensitizing chlorophyll branch intermediate, Pchlde, under darkness. Etiolated mutant seedlings display strong red fluorescence at 655 nm through UV excitation, due to Pchlde accumulation [39]. When these plants are re-exposed to light, photosensitizing Pchlde generates ¹O₂ and causes extensive photo-oxidative damage [39]. A representative transgenic line for *HvFC1* and *HvFC2* was crossed with *tigrina*^{d12}. Homozygous *tigrina*^{d12} plants were detected within a segregating F₂ population, using a

CAPS marker, designed to the causative mutation in the *FLU* gene [39] (Figure 6, 1st and 2nd panel). Lines containing *HvFC* transgenes were additionally identified by using a dominant transgene specific PCR marker (Figure 6, 3rd panel).

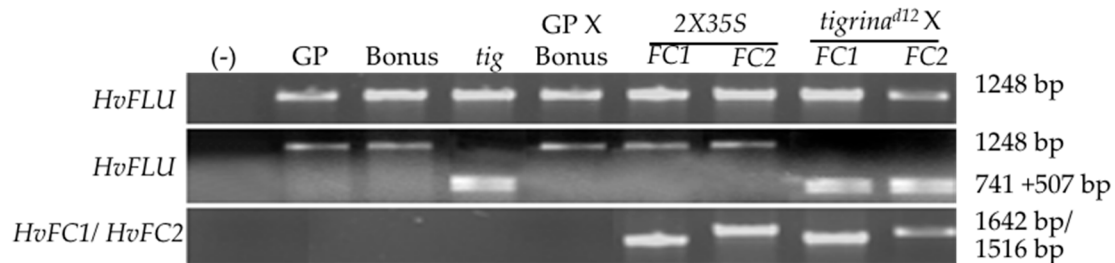


Figure 6. Molecular characterization of *tigrina*^{d12} mutants overexpressing *HvFC1* or *HvFC2* using CAPS markers and transgene specific primers. PCR was conducted using *FLU* specific primers (top panel). The PCR amplicons were cleaved using *HaeIII* restriction enzyme, and *tigrina*^{d12} mutants could be differentiated from other plants based on the cleaved fragment sizes (middle panel). The presence or absence of the transgenes was detected by using the transgene specific primers (bottom panel). Lane (-) is the negative control.

Seedlings identified to be both homozygous for *tigrina*^{d12} and containing either the *HvFC1* or *HvFC2* transgenes were compared to non-transgenic (cv. Golden Promise, cv. Bonus, *tigrina*^{d12}, Golden Promise × Bonus F₂ progenies) and transgenic controls (2 × 35S::FC1, 2 × 35S::FC2), for both Pchl_{ide} accumulation upon darkness and subsequent photo-oxidative damage induced by a continuous light treatment. Indeed, etiolated *tigrina*^{d12} seedlings displayed a strong red fluorescence (Figure 7a). However, *tigrina*^{d12} seedlings overexpressing either *HvFC1* or *HvFC2*, exhibited significantly less red fluorescence at 655 nm ($p < 0.05$), when compared to non-transgenic *tigrina*^{d12} controls (Figure 7a). Fluorescence levels were similar between the non-transgenic controls (data not presented). These findings implied that ectopic overexpression of *HvFC1* and *HvFC2* can suppress Pchl_{ide} accumulation that is normally observed in etiolated *tigrina*^{d12} seedlings.

Potential photo-toxic effects were evaluated in these plants, upon re-exposure to light, by analyzing the total chlorophyll content and the chlorophyll fluorescence parameter F_v/F_m . Total chlorophyll content was significantly reduced ($p < 0.05$) in *tigrina*^{d12} mutants, 24 h post re-illumination (Figure 7b). However, the chlorophyll content remained unchanged in transgenic *tigrina*^{d12} overexpressing either *HvFC1* or *HvFC2*, suggesting that overexpression of *HvFCs* suppress the potential photo-bleaching effects of *tigrina*^{d12}. Similarly, *tigrina*^{d12} exhibited a significant reduction in chlorophyll fluorescence, 24 h after re-illumination (Figure 7c). Such an effect was not observed in the *tigrina*^{d12} overexpressing *HvFC1*. In the *tigrina*^{d12} overexpressing *HvFC2*, F_v/F_m was reduced 24 h after re-illumination, relative to the before-dark treatment, but it was not as strong as *tigrina*^{d12}. Taken together, these results indicate that both *HvFC1* and *HvFC2* have the capacity to suppress the photo-toxic effects caused by tetrapyrrole deregulation in *tigrina*^{d12}.

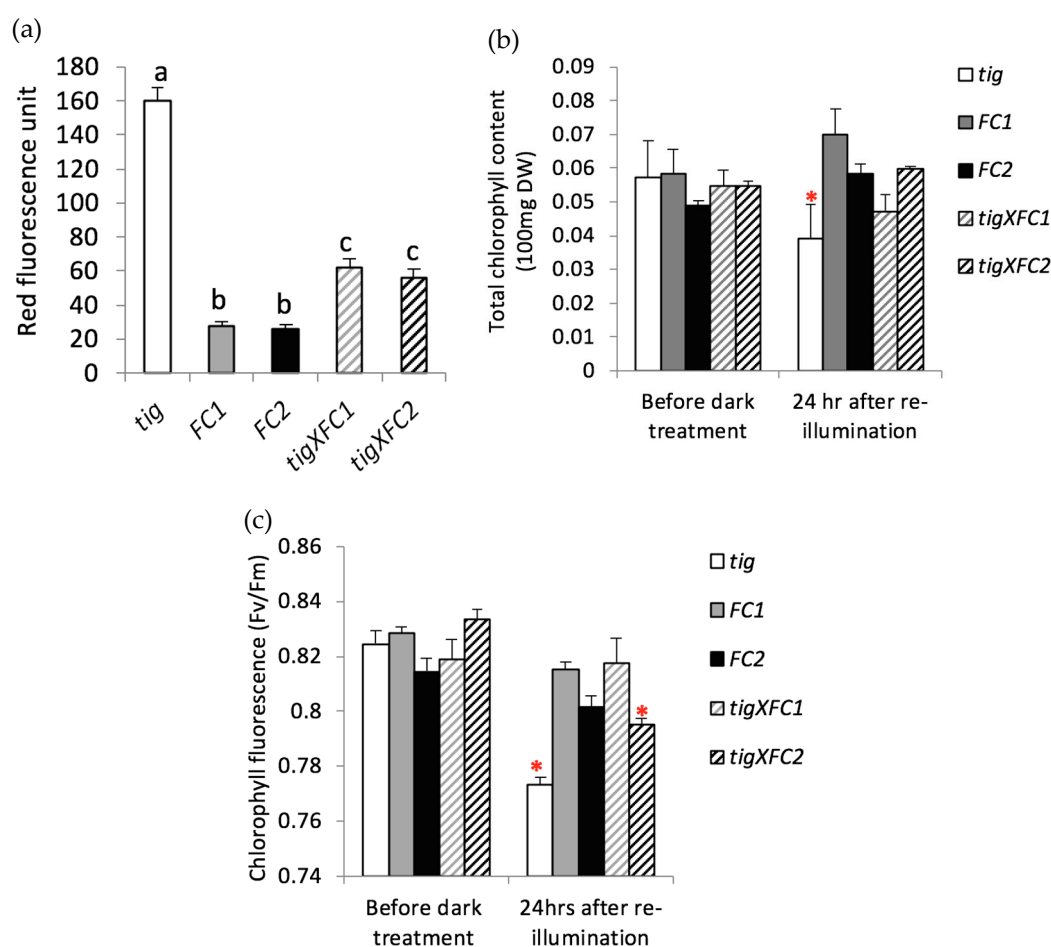


Figure 7. Ectopic overexpression of *HvFC1* and *HvFC2* suppresses *tigrina*^{d12} mutant phenotypes. (a) Red fluorescence of dark grown seedlings, which is an indication of the level of Pchlde accumulation. The data are shown as mean \pm standard error of 5 different plants. Means with the same letter are not significantly different at * $p < 0.05$ based on one-way ANOVA. (b) Total chlorophyll content and (c) Chlorophyll fluorescence (F_v/F_m) before dark treatment and upon 24 h after re-exposure to light. The data are shown as mean \pm standard error of 5 different plants. Asterisks indicate a statistically significant difference relative to before treatment, at * $p < 0.05$ based on two-way ANOVA. *tig*-*tigrina*^{d12} mutant. *FC1*, *FC2*- representative transgenic lines ectopically overexpressing either *HvFC1* or *HvFC2*. *tig* \times *FC1* or *tig* \times *FC1*-*tigrina*^{d12} mutants ectopically overexpressing either *HvFC1* or *HvFC2*.

3.5. Barley *FC1* and *FC2* are Differentially Responsive to Drought Stress and Oxidative Stress

Our results indicated that both *HvFC1* and *HvFC2* play roles in drought and oxidative stress tolerance, while previous studies reported that only *FC1* is involved in the stress defense responses [14,20–28]. Therefore, we investigated *HvFCs* stress responsive expression patterns. For this purpose, we compared well-watered control plants to plants under drought stress. Dehydrated plants were visually assessed for wilting and transcript abundance of drought responsive *Cat* and *Sod* were analyzed to ensure that the plants were successfully drought stressed. Expression of *HvFC1* and *HvFC2* was analyzed in leaves of well-watered and drought-stressed plants.

Control plants wilted 8 days post water-withholding (Figure 8a). *Cat* expression was significantly upregulated 5 days post water-withholding, relative to the well-watered plants (Figure 8b). Transcript levels of *Sod* was also significantly increased 2 to 5 days post water-withholding (Figure 8b). In-line with previous studies [16,20,21,29–34], *HvFC1* was significantly upregulated, whereas *HvFC2* was downregulated, 2 to 5 days post water-withholding, relative to the well-watered plants (Figure 8c).

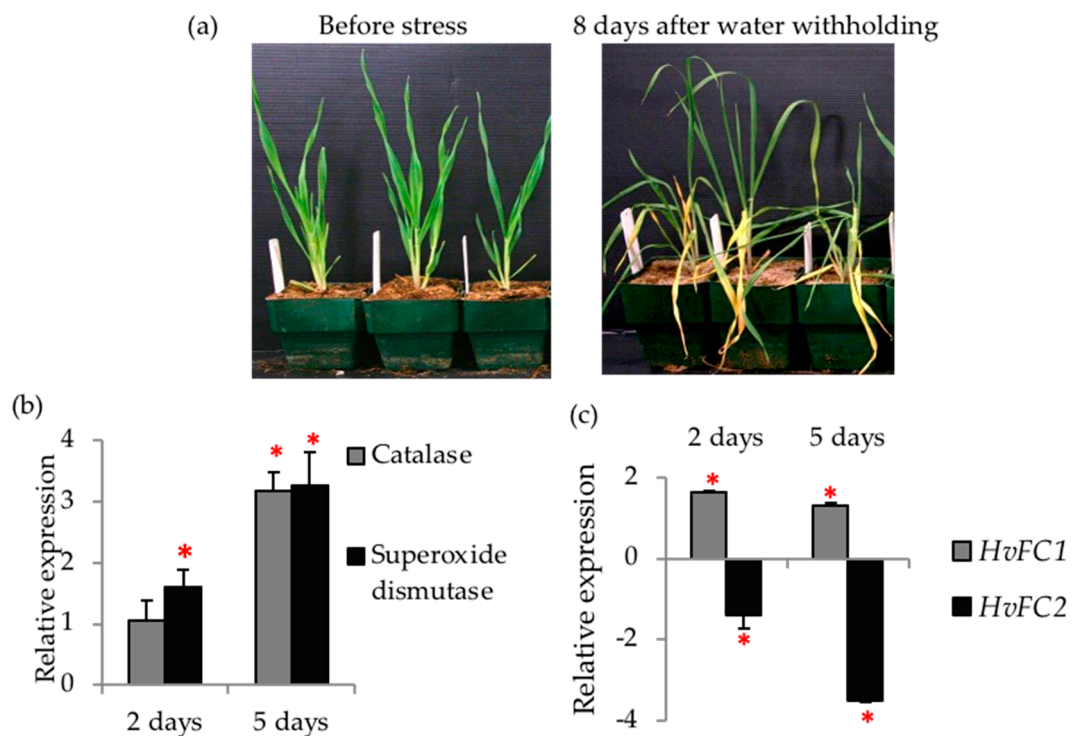


Figure 8. Transcript abundance of ROS detoxification markers (Cat and SOD) and *HvFCs* in control plants upon drought stress. (a) Phenotypes of control plants before stress and after exposure to drought stress. (b) Expression of *Cat* and *Sod* and, (c) *HvFC1* and *HvFC2* in drought-treated plants, relative to the well-watered plants. The data are shown as mean \pm standard error (SE) of 3 different plants. Asterisks indicate a statistically significant expression difference relative to the well-watered plants, at $p < 0.05$, based on one-way ANOVA.

To investigate the transcriptional responses of *HvFCs* to oxidative stress, wild-type control plants were exposed to Paraquat-induced and tetrapyrrole-mediated oxidative stress. Paraquat treated leaves were severely photo-bleached, 24 h after the treatment (Figure 9a). Even though, expression of *HvFC1* and *HvFC2* did not change 1.5 h post paraquat treatment, *HvFC1* was significantly upregulated and *HvFC2* was markedly downregulated, 24 h after paraquat application (Figure 9c). When etiolated *tigrina^{d12}* mutants were illuminated, the leaves were severely photo-bleached (Figure 9b) in response to tetrapyrrole-induced oxidative stress. Transcript levels of *HvFC1* and *HvFC2* did not significantly change 1.5 h post illumination. However, both *HvFC1* and *HvFC2* were significantly downregulated, 24 h post-illumination (Figure 9c). It is important to note that, *HvFC1* expression was less affected by severe oxidative stress than *HvFC2*, 24 h post re-illumination.

Collectively, these results demonstrate that the two *HvFCs* were differentially responsive to drought and oxidative stresses.

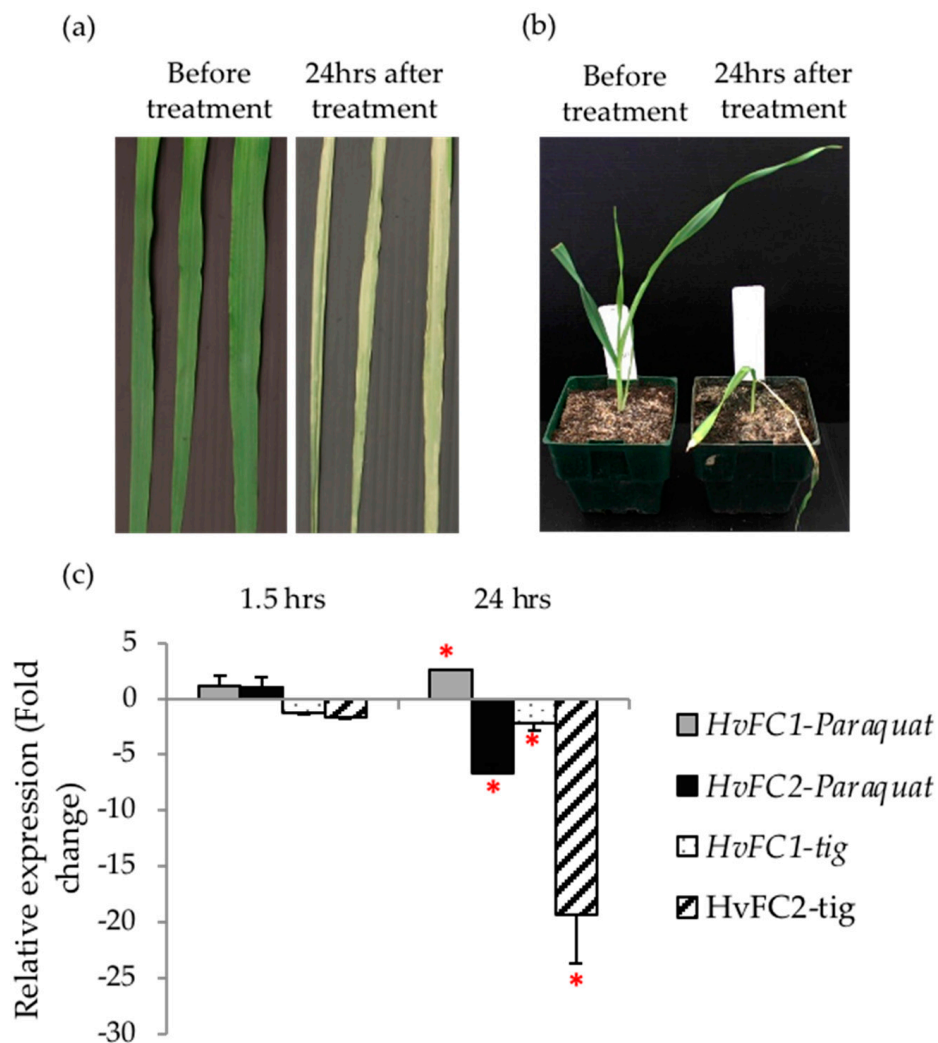


Figure 9. Phenotypes of control barley leaves and *HvFC* transcript abundance upon exposure to Paraquat-induced and tetrapyrrole-mediated oxidative stress. Leaves of control plants before and 24 h after exposure to (a) Paraquat-induced oxidative stress, and (b) tetrapyrrole-mediated oxidative stress in *tigrina*^{d12} mutants. (c) Relative expression of *HvFC1* and *HvFC2*, upon oxidative stress relative to before stress. The data are shown as mean \pm standard error (SE) of 3 different plants. Asterisks indicate a statistically significant expression difference, relative to before treatment, at $* p < 0.05$ using one-way ANOVA.

4. Discussion

4.1. Both FC1 and FC2 are Implicated in Maintaining Higher Leaf Water Status and Photosynthetic Activity Upon Drought Stress

Transgenic plants ectopically overexpressing either *HvFC1* or *HvFC2* showed several beneficial traits, which enabled them to perform better under water-limited conditions. Even though the control plants wilted at -0.6 MPa soil water potential (8 days post water-withholding), neither *HvFC1* nor *HvFC2* overexpressing transgenics exhibited wilting symptoms (Figure 3). The leaf RWC of both types of transgenics was similar to the controls, prior to stress, but they were able to maintain a higher RWC, as the soil dehydrated (Figure 4a). This finding was in agreement with Allen et al., (2015) [31] who reported that *Arabidopsis* plants overexpressing either *FC1* or *FC2* were less wilted under terminal drought. As drought stress progressed, water uptake from the soil became more difficult, because of the reducing soil water potential. This, in turn, caused a reduction in the intercellular

plant water potential and therefore the overall plant water status. One of the very early responses to water deficit was stomatal closure, which facilitated water retention by restricting transpiration. Even though we speculated that increased leaf RWC for both *HvFC* transgenics might be due to a lower g_s , *HvFC1* transgenics displayed significantly higher g_s , whereas *HvFC2* transgenics showed no significant increase in g_s relative to the controls (Figure 4b). Therefore, it is probable that *HvFC* transgenics express a more effective mechanism for water uptake.

HvFC ectopically overexpressing transgenics are expected to have a higher heme content. Several studies report that heme oxygenase (HO), which breaks down heme into an antioxidative compound, Biliverdin IX, is implicated in lateral root development [46–48]. Therefore, *HvFC* transgenics might have a higher amount of heme and HO activity in roots, which could facilitate root development, therefore, allowing plants to access deep-water resources, as the drought stress progresses. This hypothesis was supported by the fact that HO activity was significantly enhanced in root tissues, during drought stress [32]. Furthermore, rice transgenics ectopically overexpressing Protoporphyrinogen IX oxidase (PPO), produced more of the branch point intermediate, Proto IX, and increased FC activity, heme content, and HO activity in roots, upon drought [32]. Plants in this study were also able to maintain a higher RWC upon drought stress, relative to the non-transgenic controls. This would indicate that the heme branch intermediates might regulate mechanisms that aid in water acquisition, at low soil water potentials.

Transgenics ectopically overexpressing either *HvFC1* or *HvFC2* also exhibited a significantly higher photosynthetic capacity under both non-stressed and drought stress conditions, relative to controls (Figure 4c). This observation implied that before initiation of the drought stress, higher g_s of *HvFC* overexpressing transgenics was more likely to be a consequence of increased photosynthetic capacity. As stomata are highly responsive to intracellular CO_2 concentration [49,50], we assumed that the transgenics have a higher gradient in the partial pressure of CO_2 between the surrounding atmosphere and the inside of the leaf, as a result of an inherent higher carboxylation efficiency, thus, promoting higher g_s . However, as the drought stress progressed, even though the photosynthetic capacity remained high relative to controls, g_s progressively declined in both transgenics. Given that under drought stress, the stomata are more responsive to stress signals than intracellular CO_2 concentration [51–53], this reduction in g_s is most likely explained as a normal stress response.

As ribulose-1,5-bisphosphate carboxylase/oxygenase (Rubisco) is the primary enzyme involved in carboxylation, improved photosynthetic capacity of the transgenics could be due to either an increased Rubisco content or its activity. It was reported that ectopic overexpression of *Arabidopsis FC1* transcriptionally upregulated the expression of photosynthesis-associated nuclear genes (PhANG), such as *Rubisco* and light-harvesting complex b protein (*LHCB*), under non-stressed conditions [12–14]. In contrast, *Arabidopsis* plants overexpressing *FC2*, failed to display transcriptional upregulation of the same nuclear genes. These findings led the authors of these studies to propose that only the *FC1*-derived heme sub-pool might act as a plastid-to-nuclear signal. Subsequent studies revealed that chloroplasts also transmit such retrograde signals under stress conditions, therefore, modulating nuclear gene expression associated with stress acclimation [14,54–56]. This signal has since been termed an “operational signal” [57,58]. Whether heme is a causal agent in such a retrograde signaling process during drought exposure, is yet to be determined.

Our study goes some way to support a putative role for heme in retrograde signaling, given that overexpression of either *HvFC1* or *HvFC2*, significantly upregulates the expression of nuclear genes *Cat* and *Sod*, which each encode proteins necessary for ROS detoxification, upon prolonged drought conditions (Figure 5). Future investigations are required to determine whether these observations are a direct or indirect consequence of heme accumulation and signaling. If heme is deemed a bona fide retrograde signal, then our data would suggest that both *FC*-derived heme sub-pools could potentially act as operational signals to protect plants from drought-mediated cellular damage. In this context, we would anticipate transcriptional upregulation of photosynthesis-associated nuclear genes in *HvFC* transgenics, which could in part explain the observed higher photosynthetic capacity both under

well-watered and drought stress conditions. Two likely downstream targets for this signaling are *Rubisco* and *LHCB*, with *Rubisco* being a major target for improving photosynthetic capacity [59], and *LHCB*, encoding apoproteins required for binding major light harvesting pigments, such as chlorophylls and xanthophylls in photosystem II (PSII) [60,61]. It is also important to note that *LHCB* is involved in modulating g_s under drought stress and preventing oxidative damage [62,63], which could explain the improvement in photo-oxidative damage protection of *HvFC* transgenics, relative to controls.

Carbon assimilation depends on a number of factors such as the amount of light harvesting pigments, capacity for CO₂ diffusion from ambient air to the site of carboxylation and carboxylation efficiency [64,65]. *HvFC* transgenics maintained higher A_{sat} , relative to controls, under both non-stressed conditions as well as at 2 and 5 days post water-withholding (Figure 4d). This observation correlated well with the higher photosynthetic capacity and chlorophyll content for both *HvFC* transgenics (Figure 4c,e) and the higher g_s in *HvFC1* overexpressing transgenics (Figure 4b). Higher A_{sat} in the transgenics could partly be attributed to the higher chlorophyll content, which allowed more light perception for photosynthesis. In line with our results, Fan et al., [28] also found an increased chlorophyll accumulation in *AtFC1* ectopic overexpression line. Another possible reason could be due to a likely increase in heme content, resulting from *FC* overexpression. Heme being an integral component of the cytochrome *b6f* complex, is important for the photosynthetic electron transport [9,10]. Lack of cytochrome *b6f*-bound heme in *FC2* knock out *Arabidopsis* mutants, display impaired electron transport and PSII efficiency [16]. Therefore, *HvFC2* overexpressing transgenics might contain a higher cytochrome *b6f*-bound heme, therefore, improving photosynthetic electron transport capacity and PSII efficiency. *FC1* knock out *Arabidopsis* mutants, on the other hand, do not display such a reduction in photosynthetic performance, implying that *FC1*-derived heme might not necessarily be as important for photosynthesis [16]. This contrasts with our previous report showing that both *HvFC1* and *HvFC2* overexpressing transgenics improved the photosynthetic rate and photosynthetic capacity under non-stressed conditions [35]. We, therefore, expect that both *FC*-derived heme pools, were likely to contribute to photosynthetic performance, as a consequence of improved electron transport and PSII efficiency. Since both types of *HvFC* transgenics also significantly improved photosynthetic performance under drought stress, this would support the proposal that both *FCs* play an important role in adapting photosynthesis to water stress.

4.2. Both *FC1* and *FC2* Prevent Tetrapyrrole-Mediated Oxidative Stress

Under stress, photosensitizing tetrapyrrole intermediates accumulate, leading to an oxidative burst [44,45]. A study by Sobotka et al., (2011) [66] indicates that *FC2* plays an important role in preventing toxic intermediate accumulation. This evidence prompted us to investigate whether two *HvFCs* have distinct regulatory functions in preventing potential photo-oxidative damage upon stress. Here, we used the *tigrina*^{d12} mutant, which is defective in the FLU-based negative regulation of chlorophyll biosynthesis. Consequently, the etiolated mutant displayed a strong red fluorescence, which is an indicator of Pchlide accumulation (Figure 7a). Notably, overexpression of either *HvFC1* or *HvFC2*, significantly reduced toxic intermediate accumulation (Figure 7a). When etiolated mutants are illuminated, they exhibited severe photo-bleaching, indicating a significant damage to PSII, upon illumination (Figure 7b,c). However, *tigrina*^{d12} ectopically overexpressing either *HvFC1* or *HvFC2*, showed reduced photo-bleaching, indicating a suppression of photo-oxidative damage. This data suggest that both *FC1* and *FC2* play roles in preventing photo-oxidative damage caused by tetrapyrrole accumulation.

In line with these observations, the *Arabidopsis flu* mutant, an ortholog of barley *tigrina*^{d12} also shows suppressed Pchlide accumulation, when introduced into heme accumulating *hy1* or *ulf3* [67]. Therefore, a reason for the reduced intermediate levels in *HvFC* overexpressing *tigrina*^{d12} could be the increased heme content. Heme serves as a negative regulator of the tetrapyrrole biosynthesis, by inhibiting the activity of the first rate-limiting enzyme, glutamyl-tRNA reductase (GluTR), by binding to its C-terminal end [59]. Taken together, our results indicate that a likely heme-based negative feedback

mechanism protects plants from potential photo-oxidative damage under stress. This proposed role for heme is further supported by a more recent study by Kim et al. (2014) [33], who showed that ectopic overexpression of *Bradyrhizobium japonicum* cytosol-targeted FC in rice, substantially increased FC activity, total heme content, and tolerance to oxidative and polyethylene glycol-induced drought stress.

4.3. FC1 and FC2 are Differentially Responsive to Drought Stress and Oxidative Stress

Even though our study indicated that both FC1 and FC2 are good candidate genes for improving drought and oxidative stress tolerance, previous studies proposed that only FC1 is implicated in stress defense responses [29–34]. This was proposed solely based on HvFC's differential transcriptional responses to distinct stress stimuli. In order to investigate whether the two HvFC's had contrasting stress responsive expression profiles, we analyzed transcriptional abundance in the leaves of wild-type plants, before and after exposure to drought and oxidative stress. In line with previous observations, HvFC1 was significantly upregulated upon drought stress, whereas HvFC2 was markedly downregulated at the early stage of the drought stress (2 and 5 days post water-withholding) (Figure 8c).

Similar differential expression profiles of HvFC were observed in response to Paraquat-induced oxidative stress (Figure 9c). Paraquat disrupts the electron transport system of PSI, leading to generation of superoxide radical (O_2^-), which subsequently reduces into hydrogen peroxide (H_2O_2) and the hydroxyl radical (OH^\cdot). In contrast, when etiolated *tigrina*^{d12} was illuminated, both genes were severely downregulated (Figure 9c). Severe suppression of both HvFCs might be due to the elevated toxicity of 1O_2 relative to H_2O_2 [5]. It is important to note that HvFC1 expression was less affected by the photo-toxicity of 1O_2 compared to HvFC2 (Figure 9c). Data in this study showed that FC1 and FC2 were differentially responsive to drought and oxidative stress.

Collectively, these findings suggest that, despite distinct stress responsive expression of FC1 and FC2, increasing heme biosynthesis generally improved the plant photosynthetic capacity and also allowed plants to cope better when exposed to drought and oxidative stress. Both FCs are good candidates as targets for metabolic engineering towards improved crop performance, both under non-stressed and water-limited environments. Both heme pools were likely to play important roles in triggering the regulatory machinery involved in photosynthesis per se, as well as responses to drought and oxidative stress.

5. Patent

The authors declare that a patent was filed and granted for this work (WO20160544624A1).

Supplementary Materials: The following are available online at <http://www.mdpi.com/2073-4395/10/9/1351/s1>. Figure S1: A schematic illustration of the pMDC32 constitutive expression vector used for barley transformation, which harbours a dual 35S promoter, and either HvFC1 or HvFC2; Figure S2: Standardized drying curve used in the drought assay for evaluating the physiological performance of transgenics and control plants. In order to maintain -6 MPa soil water potential for one week, the pot weight was maintained at 4150g by adding small amount of water; Table S1: Primers used in this study.

Author Contributions: Conceptualization, D.S.K.N., B.P., E.J.E., R.W., and P.L.; Methodology and Validation, D.S.K.N.; Data Curation and Analysis, D.S.K.N.; Manuscript preparation, D.S.K.N., R.W., and P.L. Funding Acquisition, R.W. and P.L. All authors have read and agreed to the published version of the manuscript.

Funding: This research was supported by the Australian Research Council, the Grains Research and Development Corporation, the Government of South Australia, the University of Adelaide and DuPont Agricultural Biotechnology, USA.

Acknowledgments: We thank Bernhard Grimm of the Institute of Biology, Humboldt University, Berlin for kindly supplying *tigrina*^{d12}, Alison Hay for generating transgenic vectors, Rohan Singh for the barley transformation, and Yuan Lee for the quantitative RT-PCR analysis. We would also like to thank Julie Hayes, Penny Tricker, and Robyn Grove for the critical comments on the manuscript.

Conflicts of Interest: The authors declare no conflict of interest.

References

1. Boyer, J.S. Plant productivity and environment. *Science* **1982**, *218*, 443–448. [[CrossRef](#)] [[PubMed](#)]
2. Chaves, M.M. Effects of water deficits on carbon assimilation. *J. Exp. Bot.* **1991**, *42*, 1–16. [[CrossRef](#)]
3. Chaves, M.M.; Flexas, J.; Pinheiro, C. Photosynthesis under drought and salt stress: Regulation mechanisms from whole plant to cell. *Ann. Bot.* **2008**, *103*, 551–560. [[CrossRef](#)] [[PubMed](#)]
4. Sagadevan, G.M.; Bienyameen, B.; Shaheen, M.; Shaun, P.; Saberi, M.; Clare, V.; Er, W.; Kershini, G.; Alice, M.; Samson, M.; et al. Physiological and molecular insights into drought tolerance. *Afr. J. Biotechnol.* **2002**, *1*, 28–38. [[CrossRef](#)]
5. De Carvalho, M.H.C. Drought stress and reactive oxygen species: Production, scavenging and signaling. *Plant Signal. Behav.* **2008**, *3*, 156–165. [[CrossRef](#)] [[PubMed](#)]
6. McWilliam, J. The dimensions of drought. In *Drought Resistance in Cereals*; Baker, F.W.G., Ed.; CAB International: Wallingford, UK, 1989; pp. 1–11.
7. Fleury, D.; Jefferies, S.; Kuchel, H.; Langridge, P. Genetic and genomic tools to improve drought tolerance in wheat. *J. Exp. Bot.* **2010**, *61*, 3211–3222. [[CrossRef](#)] [[PubMed](#)]
8. Tanaka, R.; Tanaka, A. Tetrapyrrole biosynthesis in higher plants. *Annu. Rev. Plant Biol.* **2007**, *58*, 321–346. [[CrossRef](#)]
9. Cramer, W.A.; Soriano, G.M.; Ponomarev, M.; Huang, D.; Zhang, H.; Martinez, S.E.; Smith, J.L. Some new structural aspects and old controversies concerning the cytochrome b6/f complex of oxygenic photosynthesis. *Annu. Rev. Plant Biol.* **1996**, *47*, 477–508. [[CrossRef](#)]
10. Kurisu, G.; Zhang, H.; Smith, J.L.; Cramer, W.A. Structure of the cytochrome b6/f complex of oxygenic photosynthesis: Tuning the cavity. *Science* **2003**, *302*, 1009–1014. [[CrossRef](#)]
11. Del Río, L.A. ROS and RNS in plant physiology: An overview. *J. Exp. Bot.* **2015**, *66*, 2827–2837. [[CrossRef](#)]
12. Woodson, J.D.; Pérez-Ruiz, J.M.; Chory, J. Heme synthesis by plastid ferrochelatase I regulates nuclear gene expression in plants. *Curr. Biol.* **2011**, *21*, 897–903. [[CrossRef](#)] [[PubMed](#)]
13. Woodson, J.D.; Pérez-Ruiz, J.M.; Schmitz, R.J.; Ecker, J.R.; Chory, J. Sigma factor-mediated plastid retrograde signals control nuclear gene expression. *Plant J.* **2012**, *73*, 1–13. [[CrossRef](#)] [[PubMed](#)]
14. Page, M.T.; Garcia-Becerra, T.; Smith, A.G.; Terry, M.J. Overexpression of chloroplast-targeted ferrochelatase 1 results in a genome uncoupled chloroplast-to-nucleus retrograde signalling phenotype. *Philos. Trans. R. Soc. B Biol. Sci.* **2020**, *375*, 20190401. [[CrossRef](#)]
15. Moulin, M.; Smith, A.G. Regulation of tetrapyrrole biosynthesis in higher plants. *Biochem. Soc. Trans.* **2005**, *33*, 737–742. [[CrossRef](#)]
16. Scharfenberg, M.; Mittermayr, L.; Von Roepenack-Lahaye, A.; Schlicke, H.; Grimm, B.; Leister, D.; Kleine, T.; Roepenack-Lahaye, E. Functional characterization of the two ferrochelatases in *Arabidopsis thaliana*. *Plant Cell Environ.* **2014**, *38*, 280–298. [[CrossRef](#)] [[PubMed](#)]
17. Zhao, W.T.; Feng, S.J.; Li, H.; Faust, F.; Kleine, T.; Li, L.-N.; Yang, Z.M. Salt stress-induced ferrochelatase 1 improves resistance to salt stress by limiting sodium accumulation in *Arabidopsis thaliana*. *Sci. Rep.* **2017**, *7*, 14737. [[CrossRef](#)]
18. Little, H.N.; Jones, O.T.G. The subcellular localization and properties of the ferrochelatase of etiolated barley. *Biochem. J.* **1976**, *156*, 309–314. [[CrossRef](#)]
19. Chow, K.S.; Singh, D.P.; Walker, A.R.; Smith, A.G. Two different genes encode ferrochelatase in *Arabidopsis*: Mapping, expression and subcellular targeting of the precursor proteins. *Plant J.* **1998**, *15*, 531–541. [[CrossRef](#)]
20. Nagai, S.; Koide, M.; Takahashi, S.; Kikuta, A.; Aono, M.; Sasaki-Sekimoto, Y.; Ohta, H.; Takamiya, K.-I.; Masuda, T. Induction of isoforms of tetrapyrrole biosynthetic enzymes, AtHEMA2 and AtFC1, under stress conditions and their physiological functions in *Arabidopsis*. *Plant Physiol.* **2007**, *144*, 1039–1051. [[CrossRef](#)]
21. Singh, D.P.; Cornah, J.E.; Hadingham, S.; Smith, A.G. Expression analysis of the two ferrochelatase genes in *Arabidopsis* in different tissues and under stress conditions reveals their different roles in haem biosynthesis. *Plant Mol. Biol.* **2002**, *50*, 773–788. [[CrossRef](#)]
22. Smith, A.G.; Santana, M.A.; Wallace-Cook, A.D.; Roper, J.M.; Labbe-Bois, R. Isolation of a cDNA encoding chloroplast ferrochelatase from *Arabidopsis thaliana* by functional complementation of a yeast mutant. *J. Boil. Chem.* **1994**, *269*, 13405–13413.

23. Papenbrock, J.; Mishra, S.; Mock, H.-P.; Kruse, E.; Schmidt, E.-K.; Petersmann, A.; Braun, H.-P.; Grimm, B. Impaired expression of the plastidic ferrochelatase by antisense RNA synthesis leads to a necrotic phenotype of transformed tobacco plants. *Plant J.* **2001**, *28*, 41–50. [[CrossRef](#)] [[PubMed](#)]
24. Chow, K.S.; Singh, D.P.; Roper, J.M.; Smith, A.G. A single precursor protein for ferrochelatase-I from *Arabidopsis* is imported In Vitro into both chloroplasts and mitochondria. *J. Biol. Chem.* **1997**, *272*, 27565–27571. [[CrossRef](#)]
25. Suzuki, T.; Masuda, T.; Singh, D.P.; Tan, F.-C.; Tsuchiya, T.; Shimada, H.; Ohta, H.; Amith, A.G.; Takamiya, K. Two types of ferrochelatase in photosynthetic and nonphotosynthetic tissues of cucumber: Their difference in phylogeny, gene expression, and localization. *J. Biol. Chem.* **2002**, *277*, 4731–4737. [[CrossRef](#)]
26. Hey, D.; Ortega-Rodés, P.; Fan, T.; Schnurrer, F.; Brings, L.; Hedtke, B.; Grimm, B. Transgenic tobacco lines expressing sense or antisense Ferrochelatase 1RNA show modified ferrochelatase activity in roots and provide experimental evidence for dual localization of ferrochelatase 1. *Plant Cell Physiol.* **2016**, *57*, 2576–2585. [[CrossRef](#)] [[PubMed](#)]
27. Lister, R.; Chew, O.; Rudhe, C.; Lee, M.-N.; Whelan, J. *Arabidopsis thaliana* ferrochelatase-I and II are not imported into *Arabidopsis* mitochondria. *FEBS Lett.* **2001**, *506*, 291–295. [[CrossRef](#)]
28. Masuda, T.; Suzuki, T.; Shimada, H.; Ohta, H.; Takamiya, K. Subcellular localization of two types of ferrochelatase in cucumber. *Planta* **2003**, *217*, 602–609. [[CrossRef](#)]
29. Nagahatenna, D.S.K.; Langridge, P.; Whitford, R. Tetrapyrrole-based drought stress signalling. *Plant Biotechnol. J.* **2015**, *13*, 447–459. [[CrossRef](#)]
30. Nagahatenna, D.S.K.; Whitford, R. Ferrochelatase Compositions and Methods to Increase Agronomic Performance of Plants. U.S. Patent WO2016054462A1, 7 April 2016.
31. Allen, S.M.; Luck, S.; Mullen, J.; Sakai, H.; Sivasanker, S.; Tingey, S.V.; Williams, R.W. Drought Tolerant Plants and Related Constructs and Methods Involving Genes Encoding Ferrochelatases. U.S. Patent US 2015/0284739 A1, 8 October 2015.
32. Phung, T.-H.; Jung, H.-I.; Park, J.-H.; Kim, J.-G.; Back, K.; Jung, S. porphyrin biosynthesis control under water stress: Sustained porphyrin status correlates with drought tolerance in transgenic rice. *Plant Physiol.* **2011**, *157*, 1746–1764. [[CrossRef](#)]
33. Kim, J.-G.; Back, K.; Lee, H.Y.; Lee, H.-J.; Phung, T.-H.; Grimm, B.; Jung, S. Increased expression of Fe-chelatase leads to increased metabolic flux into heme and confers protection against photodynamically induced oxidative stress. *Plant Mol. Biol.* **2014**, *86*, 271–287. [[CrossRef](#)]
34. Espinas, N.A.; Kobayashi, K.; Sato, Y.; Mochizuki, N.; Takahashi, K.; Tanaka, R.; Masuda, T. Allocation of heme is differentially regulated by ferrochelatase isoforms in *Arabidopsis* cells. *Front. Plant Sci.* **2016**, *7*, 1326. [[CrossRef](#)]
35. Nagahatenna, D.S.K.; Tiong, J.; Edwards, E.J.; Langridge, P.; Whitford, R. Altering tetrapyrrole biosynthesis by overexpressing Ferrochelatases (FC1 and FC2), improves photosynthesis in transgenic barley. *J. MDPI Agron.* **2020**. (submitted).
36. Tingay, S.; McElroy, D.; Kalla, R.; Fieg, S.; Wang, M.; Thornton, S.; Brettell, R. *Agrobacterium tumefaciens*-mediated barley transformation. *Plant J.* **1997**, *11*, 1369–1376. [[CrossRef](#)]
37. Matthews, P.R.; Wang, M.; Waterhouse, P.M.; Thornton, S.; Fieg, S.J.; Gubler, F.; Jacobsen, J.V. Marker gene elimination from transgenic barley, using co-transformation with adjacent twin T-DNAs' on a standard *Agrobacterium* transformation vector. *Mol. Breed.* **2001**, *7*, 195–202. [[CrossRef](#)]
38. Améglio, T.; Archer, P.; Cohen, M.; Valancogne, C.; Daudet, F.-A.; Dayau, S.; Cruziat, P. Significance and limits in the use of predawn leaf water potential for tree irrigation. *Plant Soil* **1998**, *207*, 155–167. [[CrossRef](#)]
39. Lee, K.P.; Kim, C.; Lee, D.W.; Apel, K. TIGRINA d, required for regulating the biosynthesis of tetrapyrroles in barley, is an ortholog of the FLU gene of *Arabidopsis thaliana*. *FEBS Lett.* **2003**, *553*, 119–124. [[CrossRef](#)]
40. Hiscox, J.D.; Israelstam, G.F. A method for the extraction of chlorophyll from leaf tissue without maceration. *Can. J. Bot.* **1979**, *57*, 1332–1334. [[CrossRef](#)]
41. Burton, R.A.; Jobling, S.A.; Harvey, A.J.; Shirley, N.J.; Mather, D.E.; Bacic, A.; Fincher, G.B. The genetics and transcriptional profiles of the cellulose synthase-like HvCslF Gene Family in Barley. *Plant Physiol.* **2008**, *146*, 1821–1833. [[CrossRef](#)]
42. Schmittgen, T.D.; Livak, K.J. Analyzing real-time PCR data by the comparative CT method. *Nat. Protoc.* **2008**, *3*, 1101–1108. [[CrossRef](#)]

43. Zhang, J.; Kirkham, M. Drought-stress-induced changes in activities of superoxide dismutase, catalase, and peroxidase in wheat species. *Plant Cell Physiol.* **1994**, *35*, 785–791. [[CrossRef](#)]
44. Mock, H.-P.; Heller, W.; Molina, A.; Neubohn, B.; Sandermann, H.; Grimm, B. Expression of uroporphyrinogen decarboxylase or coproporphyrinogen oxidase antisense RNA in tobacco induces pathogen defense responses conferring increased resistance to tobacco mosaic virus. *J. Boil. Chem.* **1999**, *274*, 4231–4238. [[CrossRef](#)] [[PubMed](#)]
45. Mock, H.-P.; Keetman, U.; Kruse, E.; Rank, B.; Grimm, B. Defense responses to tetrapyrrole-induced oxidative stress in transgenic plants with reduced uroporphyrinogen decarboxylase or coproporphyrinogen oxidase activity. *Plant Physiol.* **1998**, *116*, 107–116. [[CrossRef](#)]
46. Chen, Y.-H.; Chao, Y.-Y.; Hsu, Y.Y.; Hong, C.-Y.; Kao, C.H. Heme oxygenase is involved in nitric oxide- and auxin-induced lateral root formation in rice. *Plant Cell Rep.* **2012**, *31*, 1085–1091. [[CrossRef](#)]
47. Xuan, W.; Zhu, F.-Y.; Xu, S.; Huang, B.-K.; Ling, T.-F.; Qi, J.-Y.; Ye, M.-B.; Shen, W.-B. The heme oxygenase/carbon monoxide system is involved in the auxin-induced cucumber adventitious rooting process. *Plant Physiol.* **2008**, *148*, 881–893. [[CrossRef](#)] [[PubMed](#)]
48. Xu, S.; Zhang, B.; Cao, Z.-Y.; Ling, T.-F.; Shen, W.-B. Heme oxygenase is involved in cobalt chloride-induced lateral root development in tomato. *BioMetals* **2010**, *24*, 181–191. [[CrossRef](#)] [[PubMed](#)]
49. Farquhar, G.D.; Sharkey, T.D. Stomatal conductance and photosynthesis. *Annu. Rev. Plant Physiol.* **1982**, *33*, 317–345. [[CrossRef](#)]
50. Mott, K.A. Do stomata respond to CO₂ concentrations other than intercellular? *Plant Physiol.* **1988**, *86*, 200–203. [[CrossRef](#)]
51. Chaves, M.M.; Maroco, J.P.; Pereira, J.S. Understanding plant responses to drought—From genes to the whole plant. *Funct. Plant Biol.* **2003**, *30*, 239–264. [[CrossRef](#)]
52. Flexas, J.; Medrano, H. Drought-inhibition of Photosynthesis in C₃ Plants: Stomatal and non-stomatal limitations revisited. *Ann. Bot.* **2002**, *89*, 183–189. [[CrossRef](#)]
53. Flexas, J.; Bota, J.; Loreto, F.; Cornic, G.; Sharkey, T.D. Diffusive and metabolic limitations to photosynthesis under drought and salinity in C₃ plants. *Plant Boil.* **2004**, *6*, 269–279. [[CrossRef](#)]
54. Pogson, B.; Woo, N.S.; Förster, B.; Small, I. Plastid signalling to the nucleus and beyond. *Trends Plant Sci.* **2008**, *13*, 602–609. [[CrossRef](#)] [[PubMed](#)]
55. Pfannschmidt, T. Plastidial retrograde signalling—A true “plastid factor” or just metabolite signatures? *Trends Plant Sci.* **2010**, *15*, 427–435. [[CrossRef](#)] [[PubMed](#)]
56. Zhao, C.; Haigh, A.M.; Holford, P.; Chen, Z.-H. Roles of chloroplast retrograde signals and ion transport in plant drought tolerance. *Int. J. Mol. Sci.* **2018**, *19*, 963. [[CrossRef](#)] [[PubMed](#)]
57. Xiao, Y.; Savchenko, T.; Baidoo, E.E.; Chehab, W.E.; Hayden, D.M.; Tolstikov, V.; Corwin, J.A.; Kliebenstein, D.J.; Keasling, J.D.; Dehesh, K. Retrograde signaling by the plastidial metabolite MEcPP regulates expression of nuclear stress-response genes. *Cell* **2012**, *149*, 1525–1535. [[CrossRef](#)]
58. Woodson, J.D.; Chory, J. Organelle signaling: How stressed chloroplasts communicate with the nucleus. *Curr. Boil.* **2012**, *22*, R690–R692. [[CrossRef](#)]
59. Galmes, J.; Andralojc, P.J.; Kapralov, M.V.; Flexas, J.; Keys, A.J.; Molins, A.; Parry, M.A.J.; Conesa, M.A. Environmentally driven evolution of R ubisco and improved photosynthesis and growth within the C₃ genus *Limonium* (*P. lumbaginaceae*). *N. Phytol.* **2014**, *203*, 989–999. [[CrossRef](#)]
60. Jansson, S. The light-harvesting chlorophyll a/b-binding proteins. *Biochim. Biophys. Acta (BBA) Bioenerg.* **1994**, *1184*, 1–19. [[CrossRef](#)]
61. Liu, X.-G.; Xu, H.; Zhang, J.-Y.; Liang, G.-W.; Liu, Y.-T.; Guo, A.-G. Effect of low temperature on chlorophyll biosynthesis in albinism line of wheat (*Triticum aestivum*) FA85. *Physiol. Plant.* **2012**, *145*, 384–394. [[CrossRef](#)]
62. Xu, Y.-H.; Liu, R.; Yan, L.; Liu, Z.-Q.; Jiang, S.-C.; Shen, Y.-Y.; Wang, X.-F.; Zhang, D.-P. Light-harvesting chlorophyll a/b-binding proteins are required for stomatal response to abscisic acid in *Arabidopsis*. *J. Exp. Bot.* **2011**, *63*, 1095–1106. [[CrossRef](#)]
63. De Bianchi, S.; Betterle, N.; Kouril, R.; Cazzaniga, S.; Boekema, E.; Bassi, R.; Dall’Osto, L. *Arabidopsis* mutants deleted in the light-harvesting protein Lhcb4 have a disrupted photosystem II macrostructure and are defective in photoprotection. *Plant Cell* **2011**, *23*, 2659–2679. [[CrossRef](#)]
64. Flexas, J.; Niinemets, Ü.; Gallé, A.; Barbour, M.M.; Centritto, M.; Diaz-Espejo, A.; Douthe, C.; Galmés, J.; Ribas-Carbo, M.; Rodriguez, P.; et al. Diffusional conductances to CO₂ as a target for increasing photosynthesis and photosynthetic water-use efficiency. *Photosynth. Res.* **2013**, *117*, 45–59. [[CrossRef](#)] [[PubMed](#)]

65. Austin, R.B. Genetic variation in photosynthesis. *J. Agric. Sci.* **1989**, *112*, 287–294. [[CrossRef](#)]
66. Sobotka, R.; Tichy, M.; Wilde, A.; Hunter, C.N. Functional assignments for the carboxyl-terminal domains of the ferrochelatase from *synechocystis* PCC 6803: The CAB domain plays a regulatory role, and region II is essential for catalysis. *Plant Physiol.* **2010**, *155*, 1735–1747. [[CrossRef](#)] [[PubMed](#)]
67. Goslings, D.; Meskauskiene, R.; Kim, C.; Lee, K.P.; Nater, M.; Apel, K. Concurrent interactions of heme and FLU with Glu tRNA reductase (HEMA1), the target of metabolic feedback inhibition of tetrapyrrole biosynthesis, in dark and light-grown *Arabidopsis* plants. *Plant J.* **2004**, *40*, 957–967. [[CrossRef](#)] [[PubMed](#)]



© 2020 by the authors. Licensee MDPI, Basel, Switzerland. This article is an open access article distributed under the terms and conditions of the Creative Commons Attribution (CC BY) license (<http://creativecommons.org/licenses/by/4.0/>).